REGULAR PAPER

Acceleration of potential-induced degradation in crystalline Si photovoltaic modules after a lightning impulse strike

Japanese Journal of Applied Physics **62**, SK1034 (2023)
https://doi.org/10.35848/1347-4065/accc92

REGULAR PAPER

Acceleration of potential-induced degradation in crystalline Si photovoltaic modules after a lightning impulse strike

Tetsuya Kaneko[1,2*], Suy Kimsong[2], Yukiko Hara[3], Atsushi Masuda[4,5], and Masao Isomura[1,2]

[1]Department of Electrical and Electronic Engineering, Tokai University, Hiratsuka, Kanagawa 259-1292, Japan
[2]Course of Electrical and Electronic Engineering, Tokai University, Hiratsuka, Kanagawa 259-1292, Japan
[3]National Institute of Advanced Industrial Science and Technology, Tsukuba, Ibaraki 305-8568, Japan
[4]Graduate School of Science and Technology, Niigata University, Niigata 950-2181, Japan
[5]Interdisciplinary Research Center for Carbon-Neutral Technologies, Niigata University, Niigata 950-2181, Japan

*E-mail: tetsuya-kaneko@tokai-u.jp

Received January 20, 2023; revised March 16, 2023; accepted April 12, 2023; published online May 10, 2023

The potential-induced degradation (PID) is one of the significant issues in realizing low-cost electricity from photovoltaic (PV) power generation plants. In this paper, we have investigated PID in crystalline Si (c-Si) PV modules with conventional p-type multicrystalline Si solar cells after the application of lightning impulse strikes. Lightning impulses with a voltage of −40 kV were applied to the module between the shorted electrodes of the c-Si cell and the mimic aluminum frame. It is confirmed that no degradation in the electrical characteristics of the c-Si cell occurs by applying the impulse only. We have found that the PID of c-Si PV modules was accelerated by applying the impulses between a c-Si cell and a metal frame. The acceleration of PID in the module applied with a lightning impulse might be caused by the migration of Na^+ ions easily toward the c-Si cell owing to damage to the ethylene-vinyl acetate encapsulant by impulses. © 2023 The Japan Society of Applied Physics

1. Introduction

The installation of photovoltaic (PV) systems has continued to increase globally owing to the strong demand for a shift to power generation from renewable energy sources. PV power generation, which is expected to serve as one of the major electricity sources, requires achieving low electricity prices. To obtain low-cost electricity from PV power generation systems, a long-term operation of PV modules is effective, in addition to the high efficiency and low price of PV modules. Therefore, degradation of PV modules is one of the important issues.

The causes of degradation of PV modules include, for example, mechanical cracks, discoloration or delamination of the encapsulant, and corrosion of the electrodes. Furthermore, potential-induced degradation (PID) is a significant issue in PV systems. PID in PV modules is a phenomenon that results in a decrease in the maximum output power of PV modules due to the potential difference between the grounded aluminum frames of PV modules and the solar cells inside the PV modules under operation.[1,2] Therefore, the PID phenomena are a concern, especially in large-scale PV plants with relatively high operating voltage. It has been reported that PID phenomena occur not only in PV modules with conventional p-type crystalline silicon (c-Si) solar cells[3–7] but also in other types of PV modules, such as PV modules consisting of n-type homojunction Si solar cells,[8–14] Si heterojunction solar cells,[15–18] thin-film Si solar cells,[19,20] compound semiconductor solar cells.[20,21] Even in the PV modules using conventional c-Si solar cells, several origins of PID phenomena have been proposed, for instance, ion migration of Na^+ from a cover glass to c-Si cells[22–25] and charge accumulation in an anti-reflection layer of c-Si cells.[26] Moreover, environmental conditions or climate regions around a PV system installation, such as high temperature and high humidity, have the potential to lead to PID acceleration. The PID phenomena are not always irreversible degradations, but the recovery of PID has been reported.[27,28]

Lightning strikes are widely known as electrical phenomena with extremely high voltage that can cause serious damage to electrical systems. If PV plants receive lightning strikes, parts of PV modules can be applied with high impulse voltage owing to a direct lightning strike for PV systems or induced lightning nearby the systems.[29,30] The degradation of performance in PV modules by applying a lightning impulse has been reported.[31–33] Also, direct damages to PV modules such as cracking or burnout caused by a lightning strike have been observed. Meanwhile, there are only a few studies focused on the following degradation in PV modules after the introduction of lightning-induced surges. The authors have previously reported on this topic.[34] In this paper, we have investigated the acceleration phenomena of PID in c-Si PV modules after the application of a lightning impulse strike. This paper reports in detail on Ref. 34 by expanding the contents and providing additional data.

2. Experimental methods

The PV modules fabricated by hand assembling with commercially available conventional type of multicrystalline p-type silicon solar cells were used in this study. The tested PV modules consisted of one c-Si solar cell with a structure of cover glass/ethylene-vinyl acetate (EVA)/p-type multicrystalline Si solar cell/EVA/back sheet of poly(vinyl fluoride) (PVF)/poly(ethylene terephthalate) (PET)/PVF. The tested modules had a square shape with a side of 18 cm, and the size of the c-Si cells placed in the modules was 15.6 cm. The electrodes connected to the c-Si cell were pulled out using interconnector ribbons from the two opposite edges of the module. On the two opposite edges without electrodes of the module, aluminum tapes were placed as a mimic Al frame. The Al tapes at the edges of the module were continuing from the cover glass to the back sheet.

Figure 1 shows a schematic diagram of the electrical connection in the lightning impulse application for the tested module. To simulate lightning strikes, a high-voltage impulse

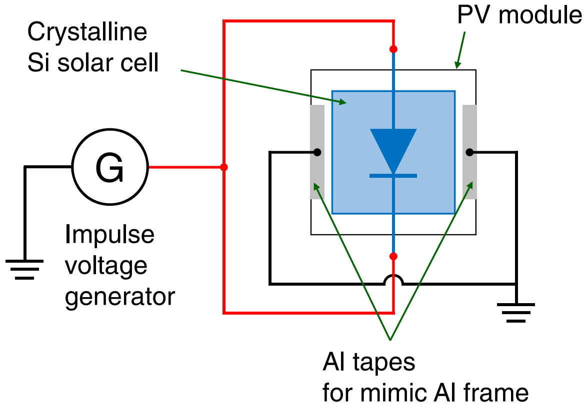

Fig. 1. Schematic diagram of electrical connection in the lightning impulse application for the tested module.

generator was utilized. Lightning impulses with a voltage of −40 kV were applied 10 times to the tested modules between the shorted electrodes of the c-Si cell and the Al tapes. The Al tapes of the modules were connected to the Earth point.

The PID tests were performed by applying a negative DC voltage of 500 V or 750 V. The voltage was applied to the shorted electrodes of the c-Si cell from a grounded Al plate with a conductive rubber sheet inserted between the cover glass of the module and the Al plate.[22] In the PID tests, the tested PV modules were kept in a thermostatic chamber at a temperature of 75 °C for 2 h.

The leakage current in PV modules reflects the conditions of insulation layers such as cover glass and EVA encapsulant. To estimate the conditions of the tested modules, the measurements in the leakage current of the modules between the cover glass and the c-Si cell in the module were carried out. The leakage current in the modules was measured at 30 °C with DC −500 V for 5 min under the same electrical connection in the PID test.

To evaluate the PID of the c-Si cell in the tested modules, the measurements of the current–voltage (*I–V*) characteristics under the dark condition were utilized. In addition, electroluminescence (EL) images of the modules were taken at some steps in the test sequence. The injection current of 4 A to the c-Si cells was used to obtain the EL images. Moreover, the voltage application of a fixed reverse bias of 4 V for 2 h to the c-Si cells was performed to understand the degradation of the cells in detail.

The test sequence in this study was as follows. Firstly, the initial results of the modules of the dark *I–V* characteristics, the leakage current, the EL images, and the current of the cells under fixed reverse voltage were obtained. The lightning impulse voltage was applied to one module, then the dark *I–V* and the leakage current measurements were performed. The PID tests with −500 V were carried out to the reference module and the impulse applied module. After the PID tests, the application of a fixed reverse bias voltage was conducted on the cells of both modules. The measurements of the dark *I–V* and the leakage current and the taking of EL images were subsequently performed. Finally, the PID tests with −750 V were carried out on both tested modules followed by the dark *I–V* measurements and EL images observation.

3. Results and discussion

3.1. Lightning impulse application

Figure 2 shows the voltage waveform of the applied lightning impulse at first and 10 times. The applied impulse voltage between the electrodes of the tested PV module and Al tapes placed on the edges of the module reaches −40 kV less than 1 μs. The impulse voltage drops rapidly around −10 kV until the next 1 μs. The overall voltage application is finished in less than 50 μs. Although the impulse voltage application onto the tested module was carried out 10 times, the applied voltage waveforms had no notable differences.

The appearance of the experimental setup around the tested module and the photo of the tested module during lightning impulse application are shown in Figs. 3(a) and 3(b). The strong electrical sparks on the surface of the module were observed between the electrodes of the cell at the edge point of the tested module and the corner of the Al tapes nearest the cell electrodes. The voltage drop shown in Fig. 2 might result from these strong sparks. In addition, it is notable that many slim sparks spread widely in the overall module, as shown in Fig. 3(b). Although only the back sheet side of the module is shown in Fig. 3(b), the sparks were also confirmed on the cover glass side of the module.

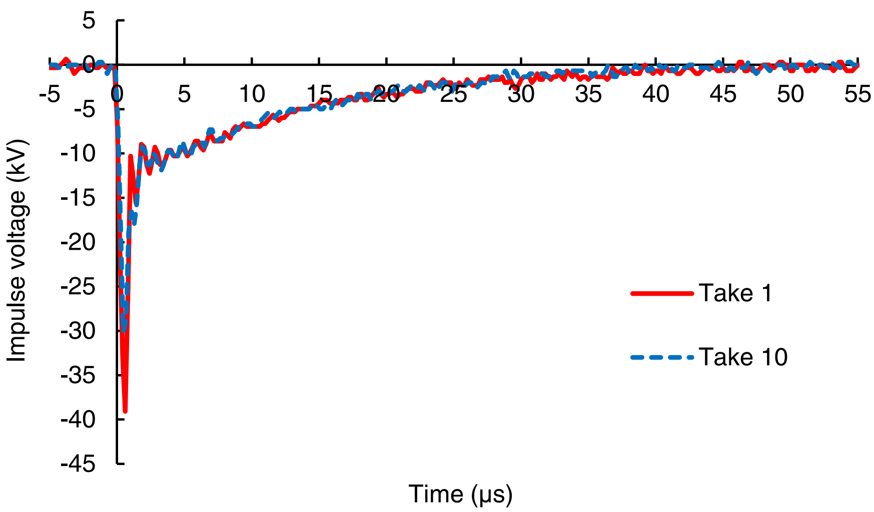

Fig. 2. The voltage waveform of the applied lightning impulse.

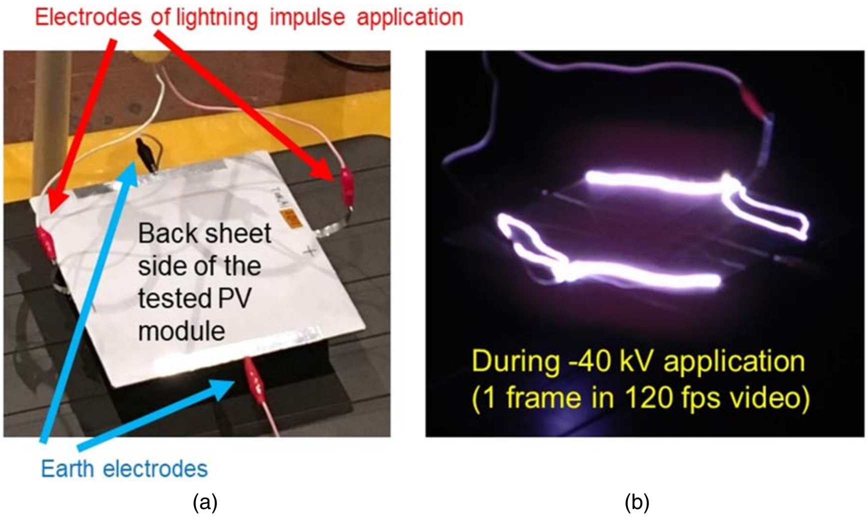

Fig. 3. Lightning impulse application. (a) Experimental setup around the tested module. (b) Sparks during lightning impulse application.

The dark *I–V* characteristics of the solar cell in the tested PV module before and after impulse application are shown in Fig. 4. It was observed that the *I–V* curve of the cell after impulse voltage application to the module was not different from the *I–V* curve of the cell at the initial.

Figure 5 shows the time dependence of current in the tested solar cell during reverse bias voltage application of −4 V before and after impulse application of 10 times. The reverse current in the cell at initial was stable for 2 h. After impulse application to the tested module, there was no change in the reverse current of the cell compared to the initial of the cell.

In the lightning impulse application, there were no effects on the dark *I–V* characteristics and the reverse current in the cell, as shown in Figs. 4 and 5. The results indicate that there is no degradation in the electrical characteristics of the c-Si cell by applying the impulse voltage of −40 kV 10 times between the frame and the cell electrodes of the PV module.

3.2. Effects of lightning impulse for PID in c-Si PV modules

Figure 6 shows the time dependence of current in the solar cells during reverse bias application of −4 V after the PID test of −500 V. In addition to the result from the tested module of impulse application, also shown in Fig. 6 is the result from the reference module with no impulse application during the reverse bias application of −4 V after the PID tests of −500 V. The time dependence of the current in both modules was obtained just after the PID test. The current of both cells at the start of the bias application indicates over 1 A, then the current decreases rapidly. Finally, the current saturates near 0.2 A until 2 h. The current of the cell in the impulse applied module shows 1.51 A at the beginning of the bias application, which is higher than that of the cell in the reference module at the beginning with 1.30 A. The saturated current at the end of the bias application for 2 h in the cell of impulse application indicates 0.153 A, which is higher than that of the cell of the reference module with 0.140 A.

The reverse current while applying −4 V in the cell before the PID test with −500 V indicated no variation with time, as shown in Fig. 5. Therefore, the origin of the variation in the reverse current shown in Fig. 6 was created by the PID test. The migration of Na^+ ions from the cover glass into the cell is the main cause of PID in modules consisting of conventional c-Si solar cells. The large reverse currents in the cells after the PID tests shown in Fig. 6 may originate from current paths caused by the Na^+ migration in the cells. The drift of

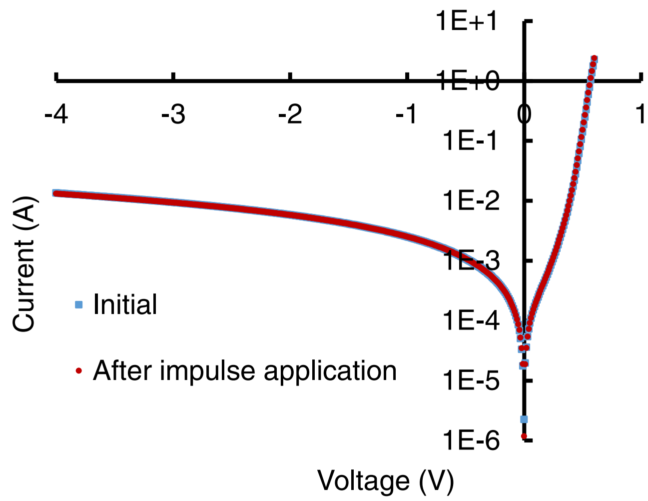

Fig. 4. Dark *I–V* characteristics of the solar cell in the tested PV module before and after impulse application of 10 times.

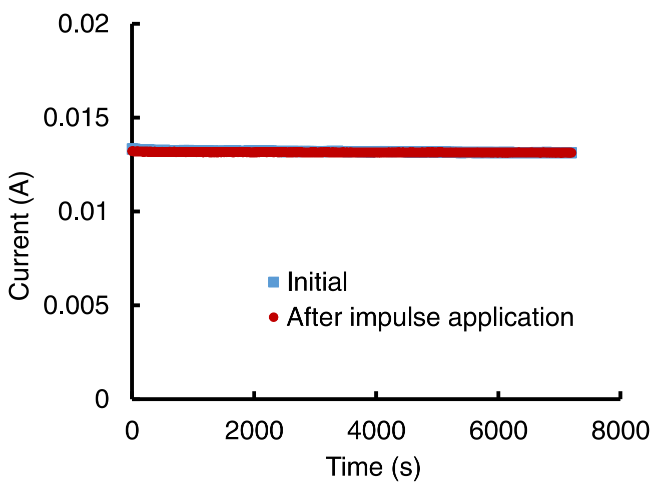

Fig. 5. Time dependence of current in the solar cell during reverse bias application of −4 V before and after impulse application.

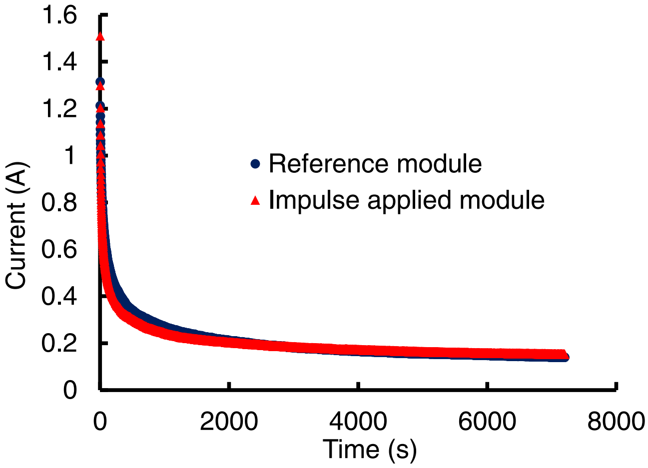

Fig. 6. Time dependence of current in the solar cells during reverse bias application of −4 V after the PID test with −500 V.

the Na^+ ions to the outside of the pn junction in the cells by applying the reverse bias voltage to the cells possibly resulted in significant drops in the reverse currents in the cells during reverse bias applications with −4 V. Additionally, the application of reverse bias to cells serves as a recovery treatment from the PID. It is assumed that the saturation current of the reverse bias application shown in Fig. 6 reflected the residual effects of the PID tests with −500 V. The large initial reverse current of 1.51 A in the cell of the impulse applied module compared to the reference cell could indicate that a greater amount of Na^+ ions reached the cell of the impulse applied module. However, the inversion of the reverse current in the reference and the impulse applied modules around 1000 s in Fig. 6 is still unclear. To understand the details, it is necessary to estimate the distribution and drift phenomena of Na^+ ions in the cell after the lightning impulse application in the future.

The dark *I–V* characteristics of the tested modules in each step of the test sequence are shown in Fig. 7. In both modules, the *I–V* characteristics of each step at the initial, the step after the PID test with −500 V followed by fixed voltage application with −4 V, and the step after the PID test with −750 V are plotted in Fig. 7. In the impulse applied module, the step after impulse application is the initial condition. Note

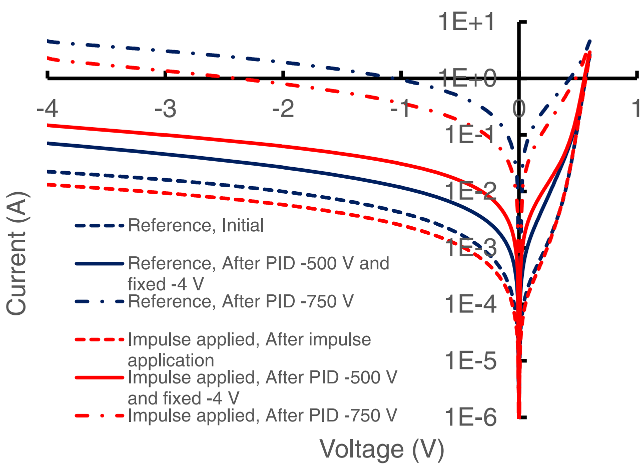

Fig. 7. Dark *I–V* characteristics of the tested modules in each step of the test sequence.

that lightning impulse application had no effect on the *I–V* characteristic of the impulse applied module, as shown in Fig. 4. In the initial condition of the modules, the reverse current of the reference module shows a larger current than the reverse current of the impulse applied module. However, a large reverse current was observed in the impulse applied module at the step after the PID test with −500 V and a fixed voltage of −4 V compared to the reference module. This means that the application of the lightning impulse voltage before the PID test accelerated the PID of the module. After the PID test with −750 V, the reverse current of the reference module became larger again than that of the impulse applied module. This result indicates that the PID of the reference module has progressed compared to the impulse applied module. The possible reason for this is discussed in a later part.

Figure 8 shows the leakage current of the tested modules at each step of the applied stresses. The difference in leakage current at the initial between both modules may result from variations in the tested modules. The leakage current of the module after impulse application increases appreciably in comparison with the initial leakage current of the same module. The lightning impulse application with −40 kV between the cell and frame mimicked by Al tapes led to an increase in the leakage current in the tested module. The result suggests that the EVA encapsulant layer was damaged by the impulse strikes. The leakage current reduction in the impulse applied module after the PID test was observed, as shown in Fig. 8. The possible reason for the reduction was a partial recovery of the damage caused by the impulse application to the module by heating during the PID test at 75 °C.

The EL images of the reference and the impulse application modules in each step of the test sequence are summarized in Fig. 9. In the EL images of the impulse applied module, no mechanical damages as cracks were observed in the EL images of the module after PID tests. The EL intensity of the modules decreased, especially in the images from the modules after the PID test with −750 V.

To clarify the intensity of EL images, histograms of the EL images were obtained. Figure 10 shows the histograms calculated from the EL images of the tested modules shown in Fig. 9. Because the histogram spectrum of the tested modules shifts toward the weak brightness side after PID tests, the PID occurred in the reference module and the impulse applied module. The spectrum shift after the PID test with −500 V followed by the fixed voltage application with −4 V in the impulse applied module seems slightly large, compared to the spectrum shift of the reference module. The findings reinforce that the PID was accelerated by applying the lightning impulse voltage of −40 kV preliminarily to the PV module. As shown in Fig. 9, the EL intensity of the cell in the impulse applied module after the PID tests decreased not a part of the cell, but over the entire area of the cell. Many slim sparks were observed throughout the module during the lightning impulse application, as shown in Fig. 3(b). Therefore, damage that led to PID acceleration caused by the impulse voltage was introduced all around the impulse applied module.

From the *I–V* characteristics and EL intensity shown in Figs. 7, 9, and 10, the cell in the reference module had lower

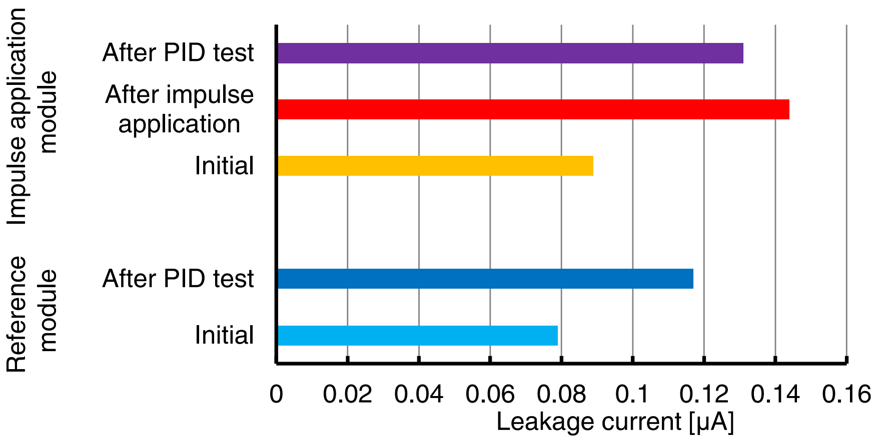

Fig. 8. Leakage current of the tested modules in each step of the test sequence.

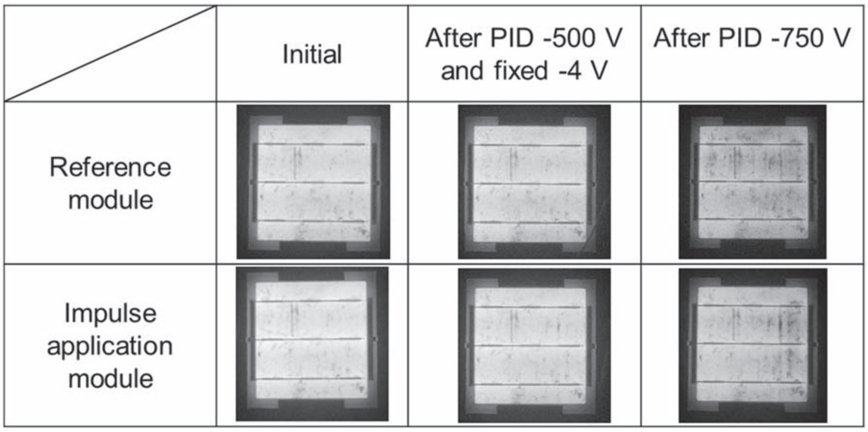

Fig. 9. EL images of the tested modules in each step of the test sequence.

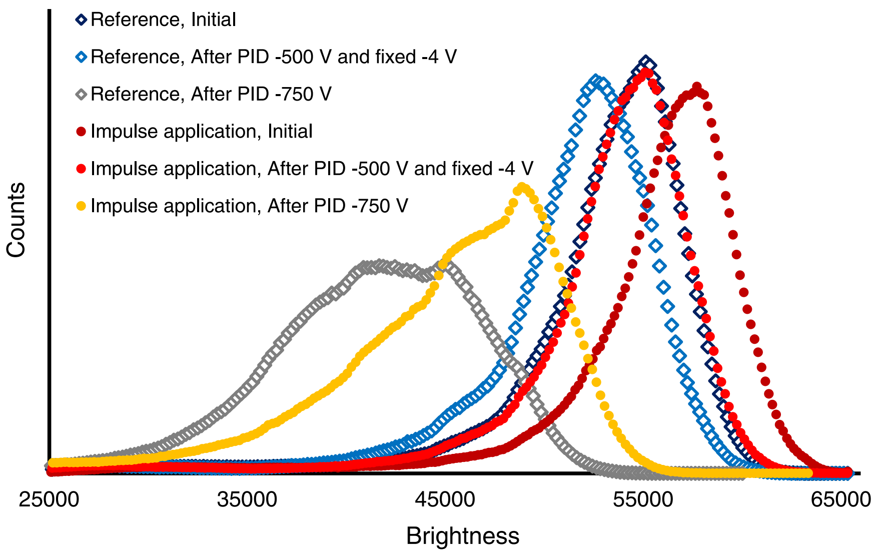

Fig. 10. Histograms of the EL images of the tested modules in each step of the test sequence.

performance and was weaker to the PID than that in the impulse application module because the larger reverse current and the lower EL intensity were observed in the initial in the reference module. The PID of the reference module was larger than the PID of the impulse applied module after the PID test with -750 V. It is believed that the relatively tough condition of the PID test with -750 V resulted in the Na^{+} migration easily to the module regardless of the lightning impulse application. Consequently, the larger PID was observed in the reference module.

By application of a lightning impulse only, there was no effect on the c-Si solar cell in the tested module, as described in Sect. 3.2. However, acceleration of PID was observed in the tested module with a lightning impulse in advance, although the applied voltage in the PID test was the relatively low voltage of -500 V, as shown in Figs. 6, 7, and 10. One of the major origins of PID phenomena in PV modules fabricated using conventional c-Si solar cells and EVA encapsulant is the migration of Na^+ ions from a cover glass to c-Si cells passing through an EVA encapsulant layer. A migration of Na^+ ions during the PID test might be much easier in the EVA encapsulant with damage by applying impulse voltage. It is conceivable that acceleration of PID in c-Si PV modules applied with lightning impulse is not caused by damage to c-Si cells but by damage to the EVA encapsulant.

4. Conclusions

It is confirmed that no degradation occurs in the electrical characteristics of the c-Si cell by applying the impulse voltage of −40 kV 10 times between the frame and the cell electrodes of the PV module. From the results of this study, we have found that the PID of c-Si PV modules was accelerated due to the application of lightning impulse voltage between a c-Si cell and the metal frame of the modules. The acceleration of PID in c-Si PV modules applied with lightning impulse might be caused by damage to the EVA encapsulant. It seems that the migration of Na^+ ions in the damaged EVA layer has been easy despite the PID test with a relatively low voltage of −500 V.

Acknowledgments

The authors would like to thank Mr. Takano and Mr. Tanabe for their support in the experiments.

ORCID iDs

Tetsuya Kaneko https://orcid.org/0000-0002-7457-8505
Atsushi Masuda https://orcid.org/0000-0003-0827-3794

1) W. Luo et al., Energy Environ. Sci. **10**, 43 (2017).
2) S. Pingel, O. Frank, M. Winkler, S. Daryan, T. Geipel, H. Hoehne, and J. Berghold, Proc. 35th IEEE Photovoltaic Specialists Conf. 2010, p. 2817, 10.1109/PVSC.2010.5616823.
3) J. Bauer, V. Naumann, S. Großer, C. Hagendorf, M. Schütze, and O. Breitenstein, Phys. Status Solidi RRL **6**, 331 (2012).
4) V. Naumann, D. Lausch, S. Großer, M. Werner, S. Swatek, C. Hagendorf, and J. Bagdahn, Energy Procedia **33**, 76 (2013).
5) V. Naumann et al., Sol. Energy Mater. Sol. Cells **120**, 383 (2014).
6) B. Ziebarth, M. Mrovec, C. Elsässer, and P. Gumbsch, J. Appl. Phys. **116**, 093510 (2014).
7) M. Wilson, A. Savtchouk, P. Edelman, D. Marinskiy, and J. Lagowski, Sol. Energy Mater. Sol. Cells **142**, 102 (2015).
8) K. Hara, S. Jonai, and A. Masuda, Sol. Energy Mater. Sol. Cells **140**, 361 (2015).
9) A. Halm, A. Schneider, V. D. Mihailetchi, L. J. Koduvelikulathu, L. M. Popescu, G. Galbiati, H. Chu, and R. Kopecek, Energy Procedia **77**, 356 (2015).
10) S. Yamaguchi, A. Masuda, and K. Ohdaira, Appl. Phys. Express **9**, 112301 (2016).
11) M. Barbato, A. Barbato, M. Meneghini, G. Tavernaro, M. Rossetto, and G. Meneghesso, Sol. Energy Mater. Sol. Cells **168**, 51 (2017).
12) S. Bae et al., Energy Sci. Eng. **5**, 30 (2017).
13) K. Hara, K. Ogawa, Y. Okabayashi, H. Matsuzaki, and A. Masuda, Sol. Energy Mater. Sol. Cells **166**, 132 (2017).
14) Y. Komatsu, S. Yamaguchi, A. Masuda, and K. Ohdaira, Microelectron. Reliab. **84**, 127 (2018).
15) S. Yamaguchi, C. Yamamoto, K. Ohdaira, and A. Masuda, Prog. Photovolt. **26**, 697 (2018).
16) A. Masuda, C. Yamamoto, Y. Hara, S. Jonai, Y. Tachibana, T. Toyoda, T. Minamikawa, S. Yamaguchi, and K. Ohdaira, Jpn. J. Appl. Phys. **59**, 076503 (2020).
17) S. Yamaguchi, C. Yamamoto, Y. Ohshita, K. Ohdaira, and A. Masuda, Sol. Energy Mater. Sol. Cells **216**, 110716 (2020).
18) J. Xu, H. T. C. Tu, A. Masuda, and K. Ohdaira, Jpn. J. Appl. Phys. **61**, SC1021 (2022).
19) A. Masuda and Y. Hara, Jpn. J. Appl. Phys. **56**, 04CS04 (2017).
20) A. Masuda, Y. Hara, Y. Shiina, S. Okamoto, and T. Okamoto, Jpn. J. Appl. Phys. **58**, SBBF07 (2019).
21) S. Yamaguchi, S. Jonai, K. Hara, H. Komaki, Y. Shimizu-Kamikawa, H. Shibata, S. Niki, Y. Kawakami, and A. Masuda, Jpn. J. Appl. Phys. **54**, 08KC13 (2015).
22) K. Hara, H. Ichinose, T. N. Murakami, and A. Masuda, RSC Adv. **4**, 44291 (2014).
23) F. Ohashi, Y. Mizuno, H. Yoshida, H. Kosuga, T. Furuya, R. Fuseya, R. J. Freitas, Y. Hara, A. Masuda, and S. Nonomura, Jpn. J. Appl. Phys. **57**, 08RG05 (2018).
24) S. Jonai, A. Tanaka, K. Muramatsu, G. Saito, K. Nakamura, A. Ogura, Y. Ohshita, and A. Masuda, Sol. Energy **188**, 1292 (2019).
25) A. Masuda, M. Akitomi, M. Inoue, K. Okuwaki, A. Okugawa, K. Ueno, T. Yamazaki, and K. Hara, Curr. Appl. Phys. **16**, 1659 (2016).
26) S. Jonai, K. Nakamura, and A. Masuda, Appl. Phys. Express **12**, 101003 (2019).
27) D. Lausch, V. Naumann, A. Graff, A. Hähnel, O. Breitenstein, C. Hagendorf, and J. Bagdahn, Energy Procedia **55**, 486 (2014).
28) A. Masuda, Y. Hara, and S. Jonai, Jpn. J. Appl. Phys. **55**, 02BF10 (2016).
29) J. C. HernÁndez, P. G. Vidal, and F. Jurado, IEEE Trans. Power Delivery **23**, 1961 (2008).
30) I. Hetita, A. S. Zalhaf, D.-E. A. Mansour, Y. Han, P. Yang, and C. Wang, Renew. Energy **184**, 134 (2022).
31) T. Jiang and S. Grzybowski, Proc. Int. Symp. Lightning Protection (XII SIPDA) 2013, p. 287.
32) T. Jiang and S. Grzybowski, Proc. Electrical Insulation Conf. 2014, p. 107.
33) T. Jiang and S. Grzybowski, ICHVE Int. Conf. on High Voltage Engineering and Application 2014.
34) S. Kimsong, T. Kaneko, Y. Hara, A. Masuda, and M. Isomura, Proc. 25th Int. Workshop on Active-Matrix Flatpanel Displays and Devices (AM-FPD) 2018, p. 1.